Applied Catalysis B: Environmental 94 (2010) 225–233

Contents lists available at ScienceDirect

Applied Catalysis B: Environmental

journal homepage: www.elsevier.com/locate/apcatb

Flow calorimetry and adsorption study of dibenzothiophene, quinoline and naphthalene over modified Y zeolites

J. Keir Thomas, Kamalakar Gunda, Peter Rehbein, Flora T.T. Ng *

Department of Chemical Engineering, University of Waterloo, 200 University Ave West, Waterloo, Canada N2L 3G1

ARTICLE INFO

Article history:
Received 14 July 2009
Received in revised form 6 November 2009
Accepted 18 November 2009
Available online 24 November 2009

Keywords:
Desulfurization
Adsorption capacity
Modified zeolites
Flow calorimetry
Heat of adsorption
Quinoline
Dibenzothiophene
Naphthalene

ABSTRACT

The adsorptive removal of dibenzothiophene (DBT), quinoline and naphthalene in hexadecane on the zeolites, NaY, NiY and CsY, using liquid phase flow calorimetry and adsorption experiments, was studied at 30 °C. NiY and CsY were prepared by the liquid phase ion-exchange method. The adsorbents were characterized by XRD, BET surface area, elemental analysis (ICP-OES) and DRIFT spectroscopic techniques. The adsorption experiments were carried out by equilibrium adsorption and flow calorimetry techniques. Modification of NaY zeolite with Ni and Cs salts resulted in the partial amorphotization of the zeolite structure which affected the adsorption properties. A higher heat of adsorption was determined for quinoline compared to DBT and naphthalene and a preferential adsorption of quinoline in a mixture containing quinoline, naphthalene and DBT was observed on NaY, NiY and CsY. The adsorption of quinoline on NiY possibly involved a direct end-on σ interaction of the Ni^{2+} with the lone pair of electrons of the N atom on quinoline while the adsorption of DBT and naphthalene occurs via a π interaction of the d orbitals of Ni^{2+} with the electrons in the aromatic rings. The equilibrium adsorption capacity of NaY was found to be the highest among the three zeolites. The decrease in the adsorption capacities of NiY and CsY appears to result mainly from the partial collapse of the zeolite structure during the ion-exchange process.

1. Introduction

The removal of sulfur from transportation fuels has been mandated by governments around the world in order to reduce atmospheric pollution by sulfur oxides [1–4]. The production of hydrogen for fuel cells also necessitated essentially sulfur free fuels, since the presence of even ultra low amounts of sulfur will poison the reforming catalyst [4,5]. The hydrodesulfurization (HDS) process is used industrially to remove the sulfur as H_2S from the sulfur-containing compounds in the transportation fuels using a catalyst and H_2 [6]. Typical catalysts used for this purpose are $CoMo/Al_2O_3$ or $NiMo/Al_2O_3$ and the reactions were conducted at elevated temperatures and pressures [7,8]. The HDS generally occurs via direct interaction between the sulfur atom and the catalyst surface, and it is therefore effective at removing sulfides, thiols and some lighter thiophenic compounds [9] where the sulfur atom is not sterically hindered by the alkyl groups on the molecule. It was found that in a low sulfur diesel fuel (433 ppmw S), the refractory sulfur species present in the highest concentrations were in the order, 4-methyl-dibenzothiophene (4MDBT) > dibenzothiophene (DBT) > 4,6-dimethyldibenzothiophene (4,6-DMDBT) > 2,3,7-trimethyl benzothiophene (2,3,7-TMBT) > 2,3,5-trimethyl benzothiophene (2,3,5-TMBT) [10]. These refractory sulfur compounds containing alkyl substituents remain even after the HDS process because the alkyl substituents hinder the direct interaction between the sulfur atom and the active site on the catalyst surface. Ma et al. found a 35-fold decrease in the HDS rate constant for 4,6-DMDBT due to the steric hindrance on the sulfur molecule [6]. Song used these rate constants to calculate the size of the catalyst bed required to achieve desulfurization down to 15 ppmw S. He determined that the volume of the catalyst bed required to reach 15 ppmw S would have to be three times larger than the catalyst bed volume required for achieving the previous requirement of 500 ppmw S in diesel fuel [11]. Other possibilities to achieve deep desulfurized fuel via HDS include increasing the hydrogen pressure fed to the reactor or increasing the reaction temperature. In order to find a cost effective solution, alternative technologies are being sought to achieve sulfur free fuels.

Among these alternative processes, the adsorptive removal of the sulfur-containing compounds by selective adsorption has received much attention. The advantages of the adsorption technique over the conventional process are milder reaction conditions since ambient temperature and pressure are used for adsorption compared to the high temperature and H_2 pressure

* Corresponding author. Tel.: +1 519 888 4567x33979; fax: +1 519 746 4979.
E-mail address: fttng@cape.uwaterloo.ca (Flora T.T. Ng).

0926-3373/$ – see front matter © 2009 Elsevier B.V. All rights reserved.
doi:10.1016/j.apcatb.2009.11.012

used for the HDS process. Moreover the properties of the sorbents, such as their adsorption capacity and selectivity are functions of the structure, morphology and composition which can be tuned with respect to the process requirements. The use of regenerable sorbents also will drastically lower the cost of the adsorption process. Various types of adsorbents, such as metal oxides, zeolites, activated carbon, clays have been tested for the adsorptive removal of the sulfur-containing compounds [12–24]. Recently our group has pioneered the study of the heat of adsorption of sulfur-containing compounds using flow calorimetry and also reported the adsorption of sulfur-containing compounds on zeolites using a DRIFT spectroscopy technique [25–27]. In the present study we focus our attention on the effect of the modification of the NaY zeolite with Ni^{2+} and Cs^{+} cations and their influence on the heats of adsorption and adsorption capacity for DBT, quinoline and naphthalene which are used as model compounds for the sulfur-containing, nitrogen-containing and the aromatic compounds present in the diesel fuel. Ni^{2+} was chosen due to the availability of the d electrons which has been reported to have a stronger interaction with DBT due to π complexation [12,13] while Cs^{+} was chosen due to its basicity and hence may be more selective to adsorb DBT in the presence of the basic quinoline.

2. Materials and methods

Dibenzothiophene (DBT), quinoline, hexadecane (anhydrous, 99%) and cesium nitrate were purchased from Aldrich. Naphthalene was obtained from BDH Laboratories. All the chemicals were used without further purification. NaY and nickel nitrate were purchased from STREM Chemicals and Fisher Scientific respectively.

2.1. Modification of NaY by ion-exchange

The powder form of the NaY zeolite was dried at 400 °C. 100 g of a 0.1 M solution of the $Ni(NO_3)_2{\cdot}6H_2O$ and $Cs(NO_3)$ were prepared in deionized water. 3 g of preheated NaY from the oven was added to the metal nitrate solution and the mixture was stirred at 80 °C for 12 h, and then cooled to room temperature. Metal modified NaY zeolite was then filtered, and the filtrate was washed with large amounts of distilled water. This ion-exchange process was repeated for two more cycles. The filtered solid paste was dried in an oven at 70 °C overnight and calcined at 400 °C for 1 h. Finally the powder was pressed, ground and sieved to 250–500 μm particle size for use in the adsorption studies.

3. Experimental procedures

3.1. Equilibrium adsorption

Adsorbate solutions of naphthalene, quinoline, and DBT dissolved in the hexadecane solvent were prepared with target concentrations of 0.5, 1, 2, 3, 5, 10, 15, 20, 25, and 30 mM. 10 g of each solution were weighed out into 3 vials (one for each zeolite). An additional 10 g of each solution was weighed out into an extra vial for each run to act as a control sample.

The zeolites were heated in a furnace at 400 °C for 2 h in order to desorb any physisorbed water that was present on the surface. Immediately after heating, 0.05 g of each zeolite was added to one vial for each of the different solutions. The vials were then placed in a shaker bath (New Brunswick Scientific Gyratory Water Bath Shaker; Model G 76) and left for 24 h at 30 °C while shaking at 170 cycles/min, in order to reach equilibrium adsorption.

After 24 h, the concentration of the adsorbate within each solution and the control sample was measured using a Varian CP-3800 gas chromatograph equipped with a VF-5MS capillary column (30 m × 0.32 mm) and three detectors and an auto-sampler. The FID detector was maintained at a temperature of 300 °C, the nitrogen specific TSD detector at 300 °C, and the sulfur specific PFPD detector at 200 °C. The initial temperature of the GC oven was 80 °C, and after injection it was immediately increased to 250 °C at a rate of 10 °C/min and held at 250 °C for 8 min to elute all the compounds in the adsorbate solution.

3.2. Heat of adsorption by flow calorimetry

The schematic diagram of the experimental setup for flow calorimetry is depicted in Fig. 1. Heats of adsorption were measured in a Setaram C80 Flow Microcalorimeter equipped with an auxiliary thermostat. The calorimeter consists of two percolation cells; one functions as a reference and the other as a sample cell. Three Teledyne ISCO D-Series high precision syringe pumps were employed for pumping the adsorbate mixture and pure solvent into the calorimeter: one pump was connected to the reference cell, and the other two pumps were connected to the sample cell via a three-way valve.

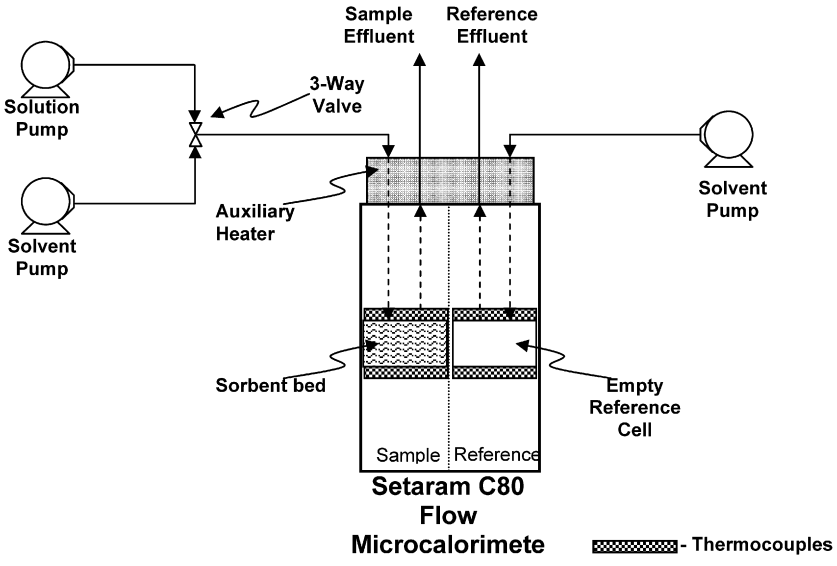

Fig. 1. Schematic diagram of the experimental setup for flow calorimetry studies.

Approximately 0.25 g of the calcined sorbent was loaded into the sample cell, which was carefully placed in the calorimeter. Pure solvent (hexadecane) was pumped through both the empty reference cell and over the adsorbent bed in the sample cell at a flow rate of 4.00 mL/h. The calorimeter and auxiliary heater were set to 30 °C to preheat the feed. All the syringe pumps and pumping lines were maintained at an isothermal temperature of 30 °C. The solvent was pumped through the calorimeter until equilibrium was reached. The equilibrium condition was characterized by a constant heat flow output ('baseline') seen in the resident Setsoft software that was integrated with the Setaram C80 Flow Microcalorimeter. The feed to the sample cell in the calorimeter was then switched to the adsorbate solution (21.8 mmol of adsorbate (DBT, quinoline or naphthalene) per litre of solution) by the three-way valve, while pure solvent continues to flow through the reference cell at the same flow rate.

As the adsorbate solution passes over the sorbent bed, the heat evolved upon the displacement of solvent by solute molecules on the adsorbent was measured by the calorimeter. Samples of the calorimeter effluent were collected periodically. The concentrations of these samples were determined by GC analysis. Recently we developed a method to calculate the amount of sorbate adsorbed based on the heat flow curve [28]. A very good agreement was obtained between the calculated value of the amount adsorbed from the heat flow measurement and the experimentally determined value based on the GC analysis of the effluent samples collected from the outlet of the calorimeter [28]. Since the experimental method to determine the amount adsorbed is based on the integration of the concentrations of all the effluent samples taken during the run, it is subject to more experimental error than the calculated value. Therefore in this paper, the amount adsorbed during the heat flow experiment was the calculated value derived from the heat flow curve [28].

4. Characterization of the adsorbents

4.1. X-Ray Diffraction

X-Ray Diffraction analysis of all the adsorbents used in the present study were carried out using a Phillips XRD instrument with a Ni filtered Cu Kα radiation with λ = 1.5404 Å. A step size of 0.01 was used from a 2θ angle of 5–40°. Samples were analyzed in the powder state with no further pre-treatment.

4.2. Surface area analysis

BET surface area of adsorbents used in the present study were measured by adsorbing nitrogen at liquid nitrogen temperature using a Micromeritics-Gemini III 2375 Surface Area analyzer after pretreating the samples initially at a temperature of 400 °C for 2 h under a helium flow.

4.3. Elemental analysis

Elemental composition of the adsorbents used in the present study was determined using Inductively Coupled Plasma Optical Emission Spectroscopy (ICP-OES) at Galbraith Laboratories, Inc. in Knoxville, Tennessee, USA.

4.4. Diffuse Reflectance Infra-Red Fourier Transform Spectroscopy (DRIFT)

The DRIFT spectra of the different adsorbents used in the present study were recorded on a Bio-Rad FTS 3000 FTIR spectrometer with a resolution of 4 cm^{-1}. The DRIFT cell is equipped with a ZnSe window and a stainless steel gas delivery line facilitated the in situ treatment of the sample under investigation. The DRIFT cell was filled with the finely powdered adsorbent and the surface of the powder was carefully smoothed and the cell was heated at 400 °C under a helium gas flow. The sample was then cooled to room temperature and pyridine was adsorbed onto it by dosing it along with the flowing helium gas as the carrier. After the saturation of the adsorbent, the sample was equilibrated for 10 min under a helium flow and then the spectra was recorded at room temperature.

Table 1
Adsorbent characterization results.

Property	Adsorbent		
	NaY	NiY	CsY
BET surface area (m^2/g)	677	524	429
Ionic radius (nm)	0.098	0.078	0.165
Al (wt%)	8.3	8.26	6.83
Si (wt%)	24.3	24.8	20.5
Na (wt%)	7.44	1.87	2.09
Cation (wt%)	–	5.59	22.8
n_{Si}/n_{Al}	2.81	2.88	2.88
Formula	Na_{33} ($Si_{89}Al_{32}O_{384}$)	$Ni_{10}Na_8$ ($Si_{91}Al_{32}O_{384}$)	$Cs_{22}Na_{12}$ ($Si_{94}Al_{33}O_{384}$)

5. Results and discussion

5.1. Surface area and XRD, and elemental analysis

The physical properties such as the BET surface area, the ionic radius of the cation and the elemental composition of the adsorbents used in this study are presented in Table 1. The X-ray diffractograms of NaY, NiY and CsY are presented in Fig. 2. The diffraction peaks at 2θ angles of 10, 12, 16 and 21° were pronounced for NaY and are in agreement with the typical XRD pattern of NaY zeolite [29], however NiY and CsY exhibited a decrease in diffraction peak intensity. This indicates that the crystalline structure of the zeolite was affected during the ion-exchange process. Similar decrease in the intensity of the XRD peaks of NiY and CsY was also observed by other workers [30,31]. It was also hypothesized that the larger cation size of the cesium will

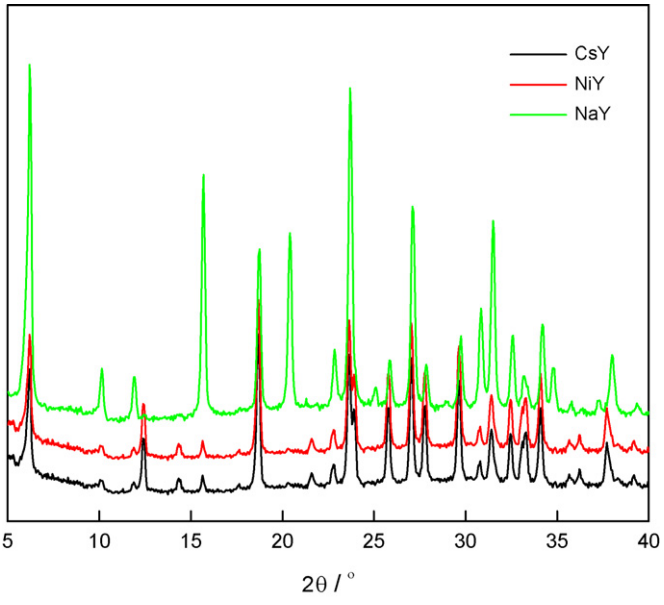

Fig. 2. XRD spectra of adsorbents used in the present study.

induce amorphotization in the crystalline structure of the NaY zeolite [30]. The intensity of the peaks at $2\theta = 6, 24, 32^\circ$ were also decreased after modification by the ion-exchange process. The decrease in peak intensity appears to be slightly greater for CsY than for NiY, indicating a greater degree of disruption of the crystalline structure. This is likely due to the higher degree of ion-exchange in CsY than in NiY. Approximately the same number of sodium ions were displaced per unit cell in both NiY and CsY. Each Ni^{2+} ion substitutes for two Na^+ ions, whereas each Cs^+ ion substitutes for each of the Na^+ ion in order to maintain charge neutrality. Thus, the concentration of Cs^+ ions in CsY is greater than Ni^{2+} ions in the NiY zeolite (Table 1). Also, the Cs^+ ion is much larger and has higher mass than the Ni^{2+} ion. Hence the resulting CsY zeolite would thus contain much more mass per unit cell than NiY which introduces strain into the zeolite structure causing the partial disruption of the crystalline structure. The decrease in the BET surface area and the extent of ion-exchange based on elemental analysis after the modification of zeolites is in agreement with the XRD results.

5.2. DRIFT analysis

The results of the adsorption of pyridine at room temperature on NaY, NiY and CsY are presented in Fig. 3. It can be observed that the Lewis adsorption sites are predominant in all the three zeolites which are in the range of 1450–1500 cm^{-1} and at the 1600 cm^{-1} region. There is a peak at 1540 cm^{-1} in the case of NiY which is attributed to the Bronsted acidity. This peak is absent in the other two adsorbents. The modification of NaY with Ni^{2+} ion imparts the Bronsted acidity to the NaY zeolite [32]. The presence of two peaks in the range of 1450 cm^{-1} in the case of NiY indicates incomplete ion-exchange of the NaY. The presence of the two peaks is more evident in NiY compared to CsY, although Cs^+ also partially substituted the Na^+ in NaY. The incomplete ion-exchange of Na^+ by Ni^{2+} and Cs^+ was also confirmed by the ICP-OES results. The new peak at about 1458 cm^{-1} in NiY may be attributed to the interaction of Ni with pyridine which was shifted towards the higher wave number compared to the NaY (1448 cm^{-1}) whereas these Lewis acid peaks are shifted very slightly towards the lower wave number in the case of CsY. This is mainly due to the difference in the electronegativities of the cations present in the zeolites where the order of electronegativity is as follows: $Cs^+ < Na^+ < Ni^{2+}$.

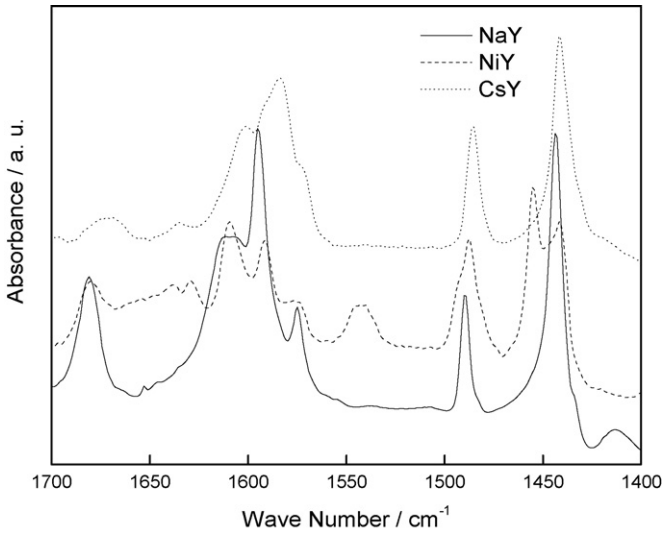

Fig. 3. DRIFT spectra of the adsorbents used in the present study.

Table 2
Adsorption of DBT/hexadecane over different adsorbents in an Equilibrium Adsorption Experiment at 30 °C.

Adsorbent	q_m (mmol/g)	K_a (L/mmol)
NaY	1.5	1.9
NiY	1.0	2.5
CsY	1.0	4.7

5.3. Equilibrium adsorption

5.3.1. Equilibrium adsorption of DBT over NaY, NiY and CsY

The results of equilibrium adsorption of DBT–hexadecane mixtures over NaY, NiY and CsY are presented in Table 2 and Fig. 4. The Langmuir adsorption model was used to describe the adsorption for all the three adsorbents. The linearized equation for the Langmuir adsorption isotherm is given by Eq. (1). The saturation equilibrium adsorption capacity (q_m) and the equilibrium adsorption constant K_a can be determined from the slope and intercept of this linearized Langmuir plot. C_e is the solution concentration of adsorbate in equilibrium with the adsorbed amount q_e.

$$\frac{C_e}{q_e} = \frac{1}{q_m} C_e + \frac{1}{K_a q_m} \quad (1)$$

The equilibrium constant K_a (column 3 of Table 2) represents the interaction between the absorbate and sorbent. A higher K_a implies that a sorbent will be more effective in removing a sorbate from a dilute solution. It can be seen from the results that q_m determined from the adsorption isotherm of the three adsorbents is in the order NaY > NiY > CsY whereas the equilibrium adsorption constant K_a is in the reverse order CsY > NiY > NaY. The higher adsorption capacity of NaY is probably due to the higher crystallinity and the higher surface area of NaY compared to that of NiY and CsY. A pore-filling mechanism for the adsorption of the refractory DBT type compounds on zeolites has been proposed by Yang and his coworkers [13] and hence a higher surface area will give a higher adsorbed amount. The equilibrium adsorption constants, K_a, are slightly higher for NiY and CsY implying that they are better suited for deep desulfurization compared to NaY. Hernandez and Yang also made a similar observation that the Ni modified Y zeolite is more effective for the adsorption of sulfur-containing compounds [12]. The lower adsorption capacity of NiY and CsY is mainly due to the partial collapse of the zeolite structure during the ion-exchange process resulting in a lower surface area.

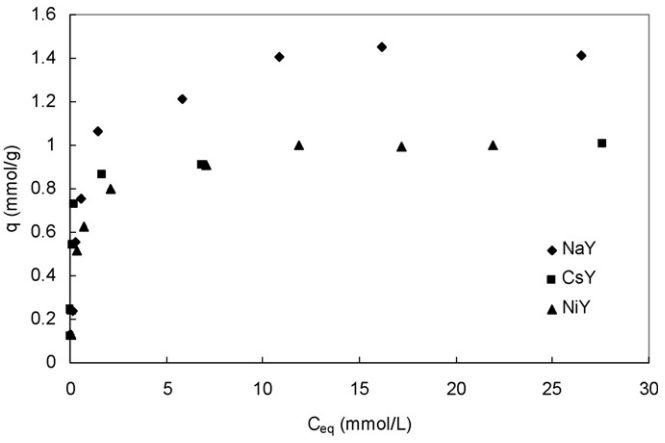

Fig. 4. Equilibrium adsorption results for the adsorption of DBT/hexadecane on different sorbents at 30 °C.

Table 3
Adsorption of naphthalene/hexadecane over different adsorbents in an Equilibrium Adsorption Experiment at 30 °C.

Adsorbent	q_m (mmol/g)	K_a (L/mmol)
NaY	1.7	1.5
NiY	1.3	1.6
CsY	1.1	3.0

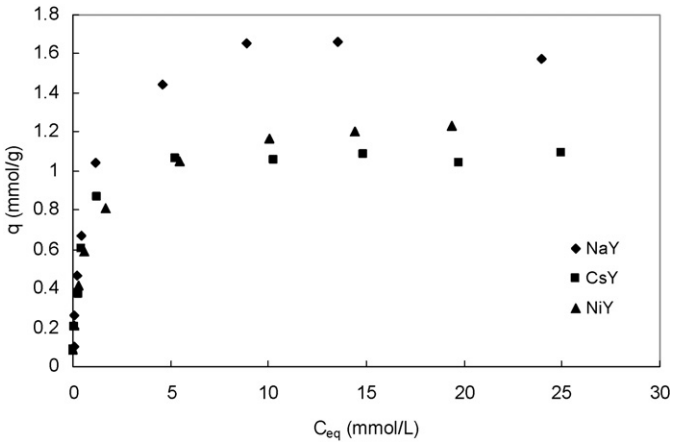

Fig. 5. Equilibrium adsorption results for the adsorption of naphthalene/hexadecane on different sorbents at 30 °C.

5.3.2. Equilibrium adsorption of naphthalene over NaY, NiY and CsY

Results of the equilibrium adsorption of naphthalene–hexadecane mixtures over NaY, NiY and CsY are presented in Table 3 and Fig. 5. The Langmuir model (Eq. (1)) was used to analyze the results. The adsorption capacity for naphthalene increases in the order of CsY < NiY < NaY. The order of the adsorption capacity for naphthalene follows the same trend as that of DBT. Therefore the decrease in the crystalline order of the modified zeolites causes a decrease in the surface area resulting in a lower amount of adsorption. Nevertheless the adsorption amount of naphthalene is significantly higher compared to that of the DBT. This is attributed to the bulkier size of the DBT compared to that of naphthalene. The equilibrium constant K_a for naphthalene follows the similar trend as that of DBT, i.e., NaY < NiY < CsY.

5.3.3. Equilibrium adsorption of quinoline over NaY, NiY and CsY

Results of the equilibrium adsorption of quinoline–hexadecane mixtures over NaY, NiY and CsY are presented in Table 4 and Fig. 6. It can be seen that the adsorption data fit the Langmuir adsorption isotherm quite well for NaY and NiY. However there was significant scatter of the data in the case of CsY. The reason for this behavior is not clear at present. It should be noted that the K_a value for CsY is much smaller than that for NiY and NaY suggesting indeed the basicity of Cs^+ caused a decrease in the K_a value and hence CsY will be less effective for the removal of quinoline from dilute solutions of quinoline compared to NiY and NaY.

An interesting observation is that the equilibrium adsorption amount of quinoline on NiY is less than half of that measured for NaY and also less than that measured for CsY. This cannot be

Table 4
Adsorption of quinoline/hexadecane over different adsorbents in an Equilibrium Adsorption Experiment at 30 °C.

Adsorbent	q_m (mmol/g)	K_a (L/mmol)
NaY	1.9	12.2
NiY	0.9	11.9
CsY	1.2	0.1

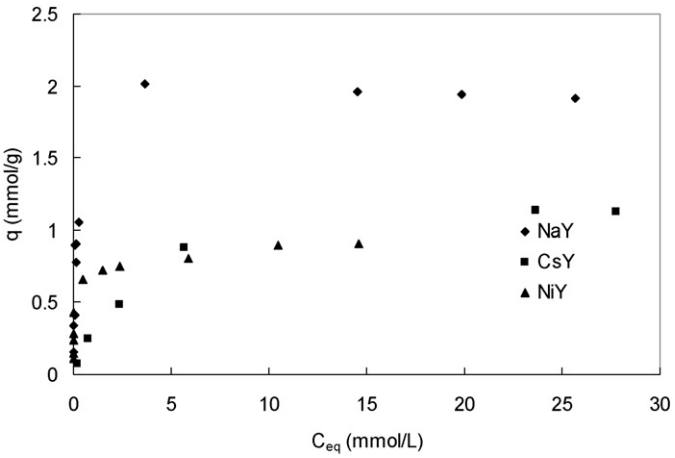

Fig. 6. Equilibrium adsorption results for the adsorption of quinoline/hexadecane on different sorbents at 30 °C.

accounted for by the differences in the size of ionic radius or the total surface area since the Cs^+ cation is larger and the surface area of CsY was found to be less than that of NaY and NiY. A possible explanation may be due to the nature of the adsorption mode of quinoline on these sorbents and will be discussed in Section 5.4.

5.4. Determination of the heats of adsorption of DBT, quinoline and naphthalene over NaY, NiY and CsY in the calorimeter

5.4.1. Heat of adsorption on NaY

The results of heats of adsorption and amounts adsorbed for NaY are presented in Table 5 and Fig. 7. The results for all the heat measurements shown in Tables 5–7 are reproducible within ±5%. It should be noted that the heat of adsorption of a particular adsorbate

Table 5
Results of heat of adsorption and amount of adsorption over NaY in the calorimeter at 30 °C (flow rate: 4 mL/h; concentration of adsorbate solution: 21.8 mM).

Adsorbate	ΔH_{Ads}		Amount adsorbed
	J/g	kJ/mol	mmol/g
DBT	34.3	28.6	1.2
Quinoline	60.2	66.9	0.9
Naphthalene	38.2	20.1	1.9

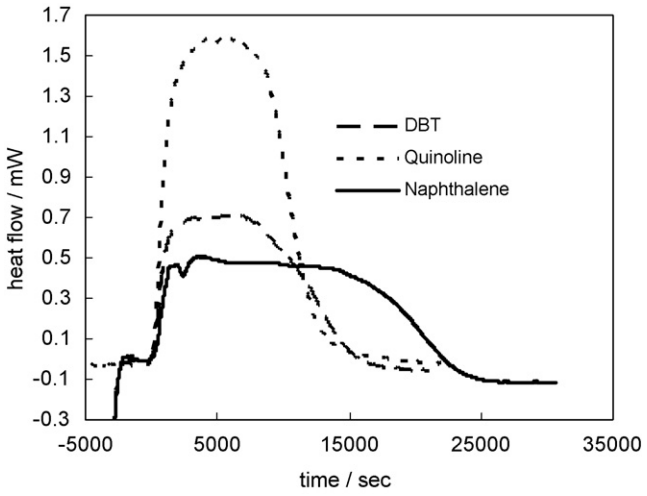

Fig. 7. Heat flow curves for DBT, quinoline and naphthalene over NaY at 30 °C (flow rate: 4 mL/h, concentration of sorbate: 21 mM).

Table 6
Results of heat of adsorption and amount of adsorption over NiY in the calorimeter at 30 °C (flow rate: 4 mL/h; concentration of adsorbate solution: 21.8 mM).

Adsorbate	ΔH_{Ads}		Amount adsorbed
	J/g	kJ/mol	mmol/g
DBT	31.2	34.6	0.9
Quinoline	60.9	101.5	0.6
Naphthalene	30.3	23.3	1.3

Table 7
Results of heat of adsorption and amount of adsorption over CsY in the calorimeter at 30 °C (flow rate: 4 mL/h; concentration of adsorbate solution: 21.8 mM).

Adsorbate	ΔH_{Ads}		Amount adsorbed
	J/g	kJ/mol	mmol/g
DBT	9.0	22.5	0.4
Quinoline	18.1	45.3	0.4
Naphthalene	22.1	24.5	0.9

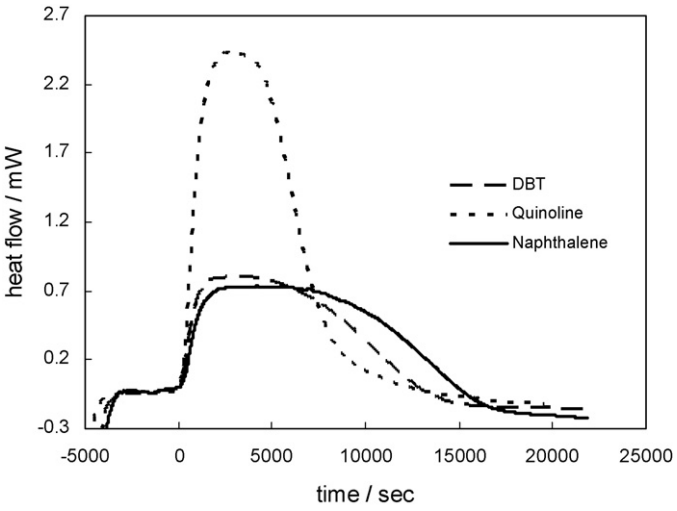

Fig. 8. Heat flow curves for DBT, quinoline and naphthalene over NiY at 30 °C (flow rate: 4 mL/h, concentration of sorbate: 21 mM).

is the heat released due to the displacement of the hexadecane molecule by that adsorbate in the liquid phase [26,27]. Furthermore the heat of adsorption measured is only an average value due to the adsorption of the sorbate on different adsorption sites on the zeolites. Heats of adsorption on NaY in kJ/mol of adsorbate follows the order: quinoline ≫ DBT > naphthalene while the adsorption amount measured in the calorimeter and the q_m values determined from the equilibrium measurements are in the opposite order: naphthalene > DBT > quinoline. This shows that a higher heat of adsorption does not necessarily lead to a higher amount of adsorption of the sorbate. The amount adsorbed is dependent on the available adsorption sites and the size of the adsorbate. It should be noted that the amount adsorbed listed in Table 5 was derived from the heat flow measurements and corresponded to the total amount adsorbed for a specific adsorbate concentration and when the heat flow curve reached a steady baseline. Hence the amounts adsorbed determined in these heat flow measurements are different from the saturation equilibrium adsorption, q_m, derived from the Langmuir plot. In addition, diffusion effects will also affect the amount adsorbed in the calorimeter. The heat of adsorption measured for the quinoline/hexadecane solution was 63.1 kJ/mol of quinoline which was much higher than that measured for DBT/hexadecane and naphthalene/hexadecane. This may be due to the stronger electrostatic interaction resulting due to the greater charge difference between the electropositive cation Na^+ and the electronegative character of the lone pair of electrons on the N atom of the quinoline. The higher heat of adsorption of quinoline on NaY compared to DBT and naphthalene indicates that quinoline will be preferentially adsorbed in a mixture containing quinoline, naphthalene and dibenzothiophene. It should also be noted that in our previous work [25] the molar heat of adsorption of DBT on NaY was 18.8 kJ/mol as compared to 28.6 kJ/mol measured in the present study. The difference in the molar heat of adsorption values was due to the difference in the properties of NaY employed in these studies. In our previous study we used NaY (n_{Si}/n_{Al} = 5.4) consisting of a binder with a surface area of 500 m^2/g whereas the NaY used in the present study does not contain a binder, has a lower Si/Al ratio (n_{Si}/n_{Al} = 2.81) and a higher surface area of 677 m^2/g. Since this heat flow measurement gives only the overall heat of adsorption for a specific adsorbent, the presence of a binder and a different Si/Al ratio of the NaY contributed to a different measured heat of adsorption.

5.4.2. Heat of adsorption on NiY

The results of the heats of adsorption and the amounts adsorbed for NiY are presented in Table 6 and Fig. 8. On NiY, it can be seen that the heat of adsorption follows a similar trend as that of NaY: quinoline ≫ DBT > naphthalene. However, the heat measured in kJ/mol for NiY is higher compared to NaY and in particular for the adsorption of quinoline. This increase in the heat of adsorption for NiY compared to NaY for DBT and naphthalene is likely due to the π interaction between the d orbitals of Ni^{2+} ion and the π molecular orbital of the aromatic rings in DBT and naphthalene as proposed by Yang and his coworkers [16,17]. It is interesting to note that the heat of adsorption of quinoline for NiY was determined to be 101.5 kJ/mol which was much higher than the value of 66.9 kJ/mol determined for NaY. In addition the q_m value for the adsorption of quinoline on NiY was 0.9 mmol/g while that for NaY was 1.9 mmol/g and 1.2 mmol/g for CsY. The much lower value of q_m on NiY suggests that the mode of adsorption of quinoline on NiY may be different than that on NaY and CsY. It is likely that quinoline is adsorbed on NiY via an end-on adsorption through the lone pair of electrons on the N atom of quinoline to the Ni^{2+} cation. The end-on type interaction between the NiY and quinoline could interfere with the pore-filling mechanism proposed for the adsorption of DBT and naphthalene and reduce the amount adsorbed. Since every Ni^{2+} replaces 2 Na^+, this may account for the low q_m value for the adsorption of quinoline on NiY. The direct σ interaction of the Ni^{+2} with the lone pairs of the electrons on the N atom of quinoline could at least partly account for the observed overall higher heat of adsorption. Indeed, a density functional theory calculation showed that quinoline is adsorbed to the Ni edge surface of a NiMoS catalyst through an end-on adsorption to the lone pair of electrons of the N atom in quinoline with high adsorption energies of 16–26 kcal mol^{-1} [33]. A recent DFT calculation on the adsorption of quinoline and CuY zeolite indicated the direct σ interaction of Cu with the N atom of quinoline is the most stable configuration [34] and the heat of adsorption was reported to be 130.9 kJ mol^{-1}. Hence it is reasonable to propose that the adsorption of quinoline on NiY occurs via an end-on adsorption contrary to the proposed π complexation between quinoline and CuY or NiY. Our previous DRIFT data on the adsorption of CuY with DBT indicated that there are more than one kind of adsorbed species on the CuY [27]. Therefore it is possible to have both direct end-on interaction and also π complexation of the quinoline occurring on the NiY zeolite. The lower heat measured in the flow calorimeter for the adsorption of quinoline on NiY compared to the DFT calculations is due to the fact that the heat of adsorption in our studies was measured in the liquid phase. Since the heat flow measurements only provide an overall measure of the heat evolved on the adsorption of sorbates

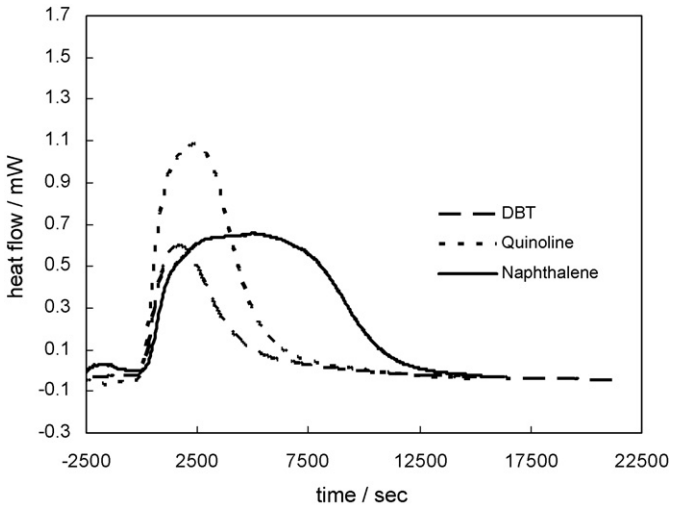

Fig. 9. Heat flow curves for DBT, quinoline and naphthalene over CsY at 30 °C (flow rate: 4 mL/h, concentration of sorbate: 21 mM).

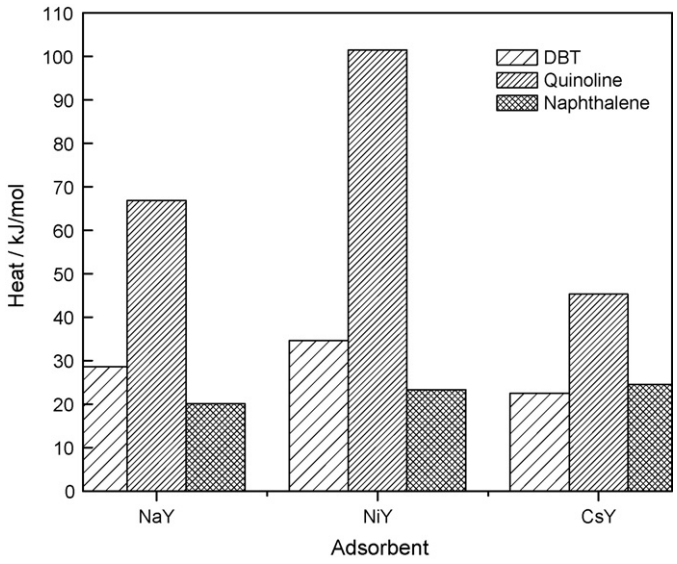

Fig. 10. Comparison of heats of adsorption on NaY, NiY and CsY.

on a particular sorbent, the data from the heat flow measurements could not provide information on the heat of adsorption on a specific adsorption site for a heterogeneous surface. In addition, it should be noted that according to our DRIFT data Bronsted acid sites are generated in the NiY zeolite which will also adsorb quinoline due to the acid–base type interaction. Regardless, our results indicate the adsorption on quinoline on NiY is very strong and hence in a mixture of DBT, quinoline and naphthalene, quinoline will be preferentially adsorbed.

5.4.3. Heat of adsorption on CsY

The results for the heats of adsorption and amounts adsorbed for CsY are presented in Table 7 and Fig. 9. The heat of adsorption of the three sorbates on CsY follow the order quinoline > naphthalene ~ DBT; however the magnitude of the heat of adsorption in each case is significantly less compared to NiY and NaY. We used Cs^+ ion in an attempt to increase the adsorption selectivity for DBT in the presence of quinoline due to the basicity of Cs^+. In spite of this, the heat of adsorption for quinoline is still higher than DBT in the CsY prepared for this study. Due to the incomplete substitution of Na^+ ion by Cs^+, the heat measured will include the contribution of the heat of adsorption of quinoline on the Cs^+ and Na^+ sites. Since the heat of adsorption of quinoline on NaY is quite high, 66.9 kJ/mol, the incomplete exchange of Na^+ by Cs^+ contributes to the apparent high heat measured on CsY.

5.4.4. Heat of adsorption on NaY, NiY and CsY

Results of the heat of adsorption of the individual adsorbates (DBT, quinoline, naphthalene) in hexadecane solution are summarized in Fig. 10. Clearly the heats of adsorption of quinoline are higher than that of DBT and naphthalene for all the three zeolites, in particular, the heat of adsorption of quinoline is significantly higher on NiY compared to NaY and CsY. It is important to note that the heat of adsorption of quinoline on CsY is significantly less than that on NaY indicating the higher basicity of Cs^+ has reduced the heat of adsorption of quinoline on Cs^+ as expected. The heat of adsorption of DBT on NiY and NaY are slightly higher than that naphthalene. It is interesting to note that Yang and his coworkers have also predicted higher heats of adsorption for sulfur compounds such as dibenzothiophene compared to aromatic hydrocarbons such as naphthalene on a CuY zeolite [35,36]. Due to the higher heat of adsorption of quinoline compared to DBT and naphthalene, these zeolites will not be selective for the adsorption of DBT in a mixture containing quinoline. It should be noted that the heat measured from flow calorimetry is an integral heat evolved due to the adsorption of the sorbate on different sites of the zeolites. Although the heat measured in flow calorimetry is not a true measure of the actual heat of adsorption of a sorbate on a specific adsorption site, it provides a relative measure of the heat of adsorption of the sorbate on a wetted sorbent. A higher heat of adsorption indicates a higher selectivity for the adsorption of that sorbate. However, a higher heat of adsorption also indicates a higher temperature will be required for the desorption and regeneration of the sorbent. Hence the heat of adsorption could be used to help in the design of selective sorbents for the production of ultra clean fuel.

6. Competitive adsorption in a flow calorimeter

6.1. Competitive adsorption of DBT, quinoline, and naphthalene on NaY

The results of the competitive adsorption experiment for all the adsorbents used in the present study are presented in Table 8. Results of the heat of adsorption from the competitive adsorption

Table 8
Summary of the competitive adsorption results of DBT, quinoline, and naphthalene in hexadecane at 30 °C.

	Heat (J/g)	Amount adsorbed (mmol/g)			Selectivity*		
		DBT	Quinoline	Naphthalene	DBT	Quinoline	Naphthalene
NaY	52.6	0.4	0.6	0.4	1	1.5	1
NiY	36.7	0.2	0.3	0.2	1	1.5	1
CsY	14.3	0.1	0.2	0.1	1	2	1

* Selectivity is defined as the ratio of the number of moles adsorbed relative to the number of moles of DBT adsorbed, equimolar (7.3 mM) solutions of each adsorbate were used for the adsorption.

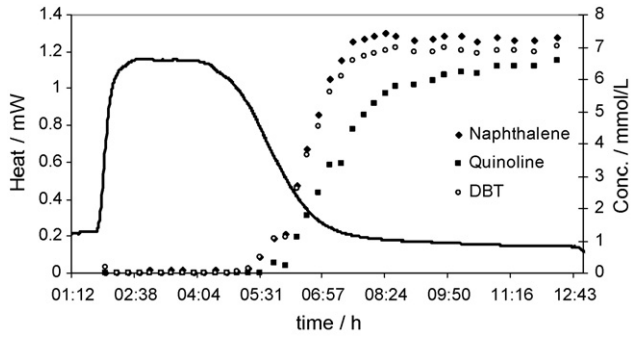

Fig. 11. Competitive adsorption of DBT, quinoline, naphthalene on NaY in hexadecane at 30 °C.

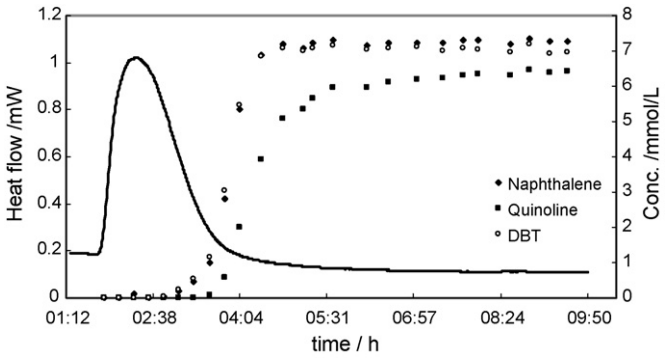

Fig. 13. Competitive adsorption of DBT, quinoline, naphthalene on CsY in hexadecane at 30 °C.

mixture DBT, quinoline, and naphthalene are presented in Fig. 11. On NaY zeolite, breakthrough of all three sorbates occurs nearly simultaneously. After breakthrough, DBT and naphthalene reach saturation much more quickly than quinoline, indicating the preferential adsorption of quinoline. Before reaching saturation, the effluent concentration of naphthalene remains slightly higher than that of DBT, indicating a slight preference for adsorption of the sulfur-containing species over naphthalene although this slight difference is within the experimental error for the determination of the concentration of the sorbates using gas chromatography. This slight preferential adsorption of DBT over naphthalene may be rationalized by the higher heat of adsorption of DBT. The effluent concentration of both naphthalene and DBT reached levels greater than their feed concentration, and began to slowly decrease to the feed concentration. This is likely due to displacement of these molecules by the more strongly adsorbed quinoline molecule. The same phenomenon has been observed in a competitive adsorption study on activated carbon and activated alumina by Kim et al. [37]. It is noted that the magnitude of this displacement is slightly greater in naphthalene than in DBT. This suggests that naphthalene is more easily displaced than DBT due to the slightly higher heat of adsorption of DBT. Therefore the DBT adsorption is slightly preferred over the naphthalene adsorption on NaY zeolite. The order of the selectivity for three different sorbate molecules follows naphthalene < DBT < quinoline, which is in agreement with the order of the measured heat of adsorption.

6.2. Competitive adsorption of DBT, quinoline, and naphthalene on NiY

Results of the heat of adsorption and the breakthrough curves from the competitive adsorption mixture are presented in Table 8 and Fig. 12. The total adsorption capacity for NiY was decreased as

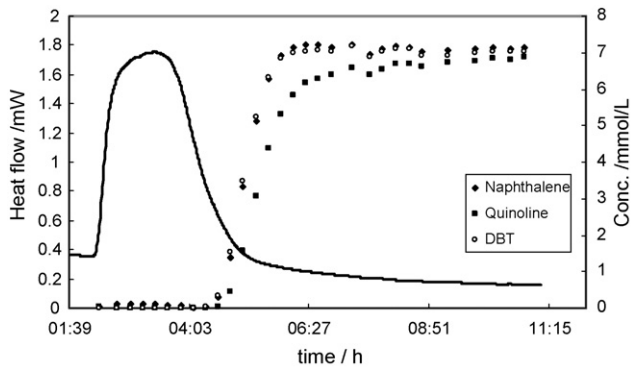

Fig. 12. Competitive adsorption of DBT, quinoline, naphthalene on NiY in hexadecane at 30 °C.

expected based on the single sorbate experiments. The selectivity towards both quinoline and naphthalene are not significantly different from that of NaY (see Table 8). Examination of the breakthrough curve shows that displacement of DBT and naphthalene does not occur to the same extent as it does on NaY zeolite. A small amount of displacement of naphthalene is observed, but almost no displacement of DBT. This may be related to the increasing strength of adsorption of DBT and naphthalene on NiY due to the π interaction between the aromatic rings and Ni^{2+}, which has the ability to back donate d-electron density to the π molecular orbital of the DBT [17].

6.3. Competitive adsorption of DBT, quinoline, and naphthalene on CsY

Results of heat of adsorption and breakthrough curves from the competitive adsorption mixture are presented in Fig. 13. As expected the adsorbed amounts of all the three sorbates are considerably lower compared to NaY and NiY adsorbents (Table 8). This follows the same trend as that of the single sorbate adsorption experiments. Again, the selectivity for quinoline is higher than DBT and naphthalene. Interestingly, it appears that selectivity for quinoline compared to DBT and naphthalene is greater for CsY compared to NiY and NaY contrary to our expectation due to the basicity of the Cs^+ (Table 8). This observed unexpected result due be attributed to the following two reasons (a) the partial substitution of the Na^+ ion by the Cs^+ ion and (b) the low amounts of sorbates adsorbed are subject to more experimental error.

7. Conclusions

Flow calorimetry is a useful technique for the determination of the relative heats of adsorption of different sorbates on a specific sorbent in the liquid phase. This relative heat of adsorption could be used to design sorbents for the selective removal of sulfur-containing compounds. Although further work is required to improve upon the technique, this study provides information on the relative heat of adsorption of DBT, quinoline and naphthalene on NaY, NiY and CsY. The heat of adsorption of quinoline is much higher than DBT and naphthalene on NaY, NiY and CsY while that for DBT is slightly higher than that for naphthalene. Our competitive adsorption experiments confirm that quinoline is preferentially adsorbed on the three zeolites while the selectivity for DBT is very similar to or slightly higher than naphthalene. There is little difference in adsorption selectivity among NaY, NiY and CsY zeolites for DBT, quinoline and naphthalene. In general, the selectivity for adsorption increases in the order; naphthalene < DBT < quinoline. This suggests that aromatics are adsorbed least strongly, followed by the sulfur-containing species. The nitrogen-containing species are preferentially adsorbed to a

greater extent. These findings indicate that sulfur removal from diesel fuel would be difficult with these sorbents since, due to the preference for quinoline adsorption and the high concentration of aromatics in the diesel fuel. The adsorption capacity of the sorbents increases in the order; CsY < NiY < NaY. The decreased capacity of the modified zeolites appears to be the result of partial disruption of the crystalline structure during the ion-exchange process. Good agreement was found between the relative heats of adsorption of sorbates employed and their selectivity with respect to each sorbent. In terms of desulfurization capability, our results indicate that the sorbents, in decreasing order of suitability, are NaY > NiY > CsY. On the basis of this work, NaY is the preferred desulfurization sorbent, since it represents the highest capacity for sulfur removal coupled with moderate heats of displacement, allowing for easier and more economical sorbent regeneration. These results differ from those in the literature which indicated an increased sulfur removal capacity for NiY over NaY. This discrepancy is likely due to degradation of the crystalline structure of our zeolites during modification by an ion-exchange process, a phenomenon not reported by other research groups on the adsorption of sulfur and nitrogen-containing compounds by modified zeolites.

Acknowledgements

Financial support from Natural Sciences and Engineering Council of Canada (NSERC) and Imperial Oil Research Grant is gratefully acknowledged.

References

[1] H. Topsøe, B.S. Clausen, F.E. Massoth, Hydro Treating Catalysis Science and Technology, Springer, Berlin, 1996, pp. 7.
[2] B.C. Gates, H. Topsøe, Polyhedron 16 (1997) 3213.
[3] C. Song, X. Ma, Catal. Today 77 (2002) 107.
[4] J.L. Sotelo, M.A. Uguina, M.D. Romero, J.M. Gomez, V.I. Agueda, M.A. Ortiz, Zeolites and mesoporous materials at the dawn of 21st century, Stud. Surf. Sci. Catal. 135 (2001) 412.
[5] D.L. King, C. Faz, T. Flynn, Soc. Automot. Eng. 1 (2000) 1.
[6] X. Ma, K. Sakanishi, I. Mochida, Ind. Eng. Chem. Res. 33 (1994) 218.
[7] T.C. Ho, Catal. Today 98 (2004) 3.
[8] M. Xue, R. Chitrakar, K. Sakane, T. Hirotsu, K. Ooi, Y. Yoshimura, Q. Feng, N. Sumida, J. Colloid Interface Sci. 285 (2005) 487.
[9] B.S. Liu, D.F. Xu, J.X. Chu, W. Liu, C.T. Au, Energy Fuels 21 (2007) 250.
[10] F. Liang, M. Lu, M.E. Birch, T.C. Keener, Z. Liu, J. Chromatogr. A 1114 (2006) 145.
[11] C. Song, Catal. Today 86 (2003) 211.
[12] A.J. Hernandez-Maldonado, R.T. Yang, Catal. Rev. 46 (2004) 111.
[13] R.T. Yang, A.J. Hernandez-Maldonado, F.H. Yang, Science 301 (2003) 79.
[14] R.T. Yang, A. Takahashi, F.H. Yang, Ind. Eng. Chem. Res. 40 (2001) 6236.
[15] A.J. Hernandez-Maldonado, R.T. Yang, Ind. Eng. Chem. Res. 42 (2003) 123.
[16] A.J. Hernandez-Maldonado, R.T. Yang, Ind. Eng. Chem. Res. 42 (2003) 3103.
[17] A.J. Hernandez-Maldonado, R.T. Yang, Ind. Eng. Chem. Res. 43 (2004) 1081.
[18] A.J. Hernandez-Maldonado, S.D. Stamatis, R.T. Yang, A.Z. He, W. Cannella, Ind. Eng. Chem. Res. 43 (2004) 769.
[19] A.J. Hernandez-Maldonado, R.T. Yang, Ind. Eng. Chem. Res. 43 (2004) 6142.
[20] A.J. Hernandez-Maldonado, R.T. Yang, AIChE J. 50 (2004) 791.
[21] S. Haji, C. Erkey, Ind. Eng. Chem. Res. 42 (2003) 6933.
[22] S.G. McKinley, R.J. Angelici, Chem. Commun. (2003) 2620.
[23] S. Velu, X. Ma, C. Song, Ind. Eng. Chem. Res. 42 (2003) 5293.
[24] A.S.H. Salem, S.H. Hamid, Chem. Eng. Technol. 20 (1997) 342.
[25] F.T.T. Ng, A. Rahman, T. Ohasi, M. Jiang, Appl. Catal. B: Environ. 56 (2005) 127.
[26] M. Jiang, F.T.T. Ng, A. Rahman, V. Patel, Thermochim. Chem. Acta 434 (2005) 27.
[27] M. Jiang, F.T.T. Ng, Catal. Today 116 (2006) 530.
[28] J. Keir Thomas, MASc Thesis, University of Waterloo, Waterloo, Ontario, Canada, 2008, pp. 37-88
[29] M.M. Treacy, J.B. Higgins, in: John B. Higgins (Ed.), Collection of Simulated XRD Powder Patterns for Zeolites, Fourth ed., Elsevier, Amsterdam, 2007.
[30] S. Yang, A. Navrotsky, Microporous Mesoporous Mater. 37 (2000) 175.
[31] P. Concepción-Heydorn, C. Jia, D. Herein, N. Pfänder, H.G. Karge, F.C. Jentoft, J. Mol. Catal. A: Chem. 162 (2000) 227.
[32] B. Coughlan, M.A. Keane, J. Catal. 123 (1990) 364.
[33] M. Sun, A.E. Nelson, J. Adjaye, Catal. Today 109 (2005) 49.
[34] D. Liu, J. Gui, Z. Sun, J. Mol. Catal. A: Chem. 291 (2008) 17.
[35] F.H. Yang, A.J. Hernandez-Maldonado, R.T. Yang, Sep. Sci. Technol. 39 (8) (2004) 1717.
[36] A. Jayaraman, F.H. Yang, R.T. Yang, Energy Fuels 20 (2006) 909.
[37] J.H. Kim, X. Ma, A. Zhou, A.C. Song, Catal. Today 111 (2006) 74.